HAL
open science

Specific heat measurements and structural investigation of CeCu6 - xSnx compounds

Olivier Isnard, E. G. Moshopoulou, J. Prchal, P. Javorsky

To cite this version:

Olivier Isnard, E. G. Moshopoulou, J. Prchal, P. Javorsky. Specific heat measurements and structural investigation of CeCu6 - xSnx compounds. Journal of Physics: Condensed Matter, 2010, 22, pp.5602. 10.1088/0953-8984/22/43/435602 . hal-00978115

HAL Id: hal-00978115

https://hal.science/hal-00978115v1

Submitted on 26 Apr 2014

HAL is a multi-disciplinary open access archive for the deposit and dissemination of scientific research documents, whether they are published or not. The documents may come from teaching and research institutions in France or abroad, or from public or private research centers.

L'archive ouverte pluridisciplinaire **HAL**, est destinée au dépôt et à la diffusion de documents scientifiques de niveau recherche, publiés ou non, émanant des établissements d'enseignement et de recherche français ou étrangers, des laboratoires publics ou privés.

Specific heat measurements and structural investigation of $CeCu_{6-x}Sn_x$ compounds

O. Isnard[1], E. G. Moshopoulou[1,2], J. Prchal[3], P. Javorsky[3]

[1]*Institut Néel, CNRS / Université Joseph Fourier de Grenoble, 25 Avenue des Martyrs, BP166X, F-38042 Grenoble Cédex 9, FRANCE*

[2]*Institute of Materials Sciences, National Center of Scientific Research "Demokritos" 15310, Agia Paraskevi, GREECE*

[3]*Charles University, Faculty of Mathematics and Physics, Department of Condensed Matter Physics, Ke Karlovu 5, 12116 Prague 2, The Czech Republic*

Abstract

The evolution of the crystal structure and some magnetic properties of the heavy fermion material $CeCu_{6-x}Sn_x$ (x = 0, 0.25, 0.65, 0.75, 0.85 and 1.0) has been studied by powder neutron diffraction and by specific heat measurements. The substitution of Cu by Sn suppresses the temperature induced orthorhombic to monoclinic transition, known to occur in the pure $CeCu_6$ phase. No structural phase transition has been observed in these samples as a function of x but the cell volume increases considerably in an anisotropic way. Sn occupies preferentially the special Cu crystallographic site which is next to each of the four Ce atoms in the unit cell. The transition to antiferromagnetic order, characterising the samples with higher x, is sensitive to both x and magnetic field. The results are discussed in the context of the competition between Kondo and RKKY interactions in disordered or not heavy-fermion systems and reveal an interesting interplay between composition, structure and magnetism in $CeCu_{6-x}Sn_x$.

PACS: 61.05.F- Neutron diffraction and scattering, 75.40.-s Critical-point effects, specific heats, short-range order, 75.30.Mb Valence fluctuation, Kondo lattice, and heavy-fermion phenomena

Keywords: crystal structure, Kondo interactions, heavy fermion, specific heat

E-mail: olivier.isnard@grenoble.cnrs.fr, evagelia@ims.demokritos.gr, prchal@karlov.mff.cuni.cz, javor@mag.mff.cuni.cz

1. Introduction

$CeCu_6$ is a well-known heavy-fermion material characterised by an exceptionally high electronic contribution (γ) to the specific heat of about 1.6 J/mol K^2 for single crystals at $T = 0$ K (ref. 1) and Fermi liquid behaviour. Since its discovery in 1984 (ref. 1) it has been extensively investigated; especially its physical properties were probed down to 250 μK. The material does not superconduct but below 1.5 K it exhibits temperature independent magnetic correlations (ref. 2) and it orders antiferromagnetically at 2 mK (ref. 3). $CeCu_6$ is characterised by a rather unusual for a heavy-fermion material, structural phase transition from an orthorhombic crystal structure (space group P*nma*) at room temperature (RT) to a monoclinic structure (s. g. $P2_1/c$) at around 230 K with a monoclinic angle of $\beta \approx 91.58°$ (ref. 4, 5, 6). Since such transition was also found in the non-magnetic analogue $LaCu_6$ at much higher though temperature (around 490 K) (ref. 6), it was concluded that electronic effects involving the 4*f* electrons are not responsible for the structural phase transition, i.e. the lattice degrees of freedom are not related to the heavy-fermion properties of $CeCu_6$.

Interestingly, Au-doped $CeCu_6$ exhibits different behaviour from its parent compound. Since the Au atoms are larger than the Cu ions, the crystalline lattice expands and therefore substitution of Cu by Au in $CeCu_6$ is equivalent to negative chemical pressure on the lattice. The system $CeCu_{6-x}Au_x$ exhibits long-range antiferromagnetic order at $x_c \leq x \leq 1$, where $x_c = 0.1$, below Néel temperature, T_N, ranging from ~ 0 K (for $x_c = 0.1$) to 2.3 K (for $x = 1$) (ref. 7). Especially the material $CeCu_{5.9}Au_{0.1}$ has been extensively investigated over the past twenty years because, while it is metallic, it exhibits non-Fermi liquid properties: linear resistivity between 0.2 and 0.8 K, logarithmic specific heat between 0.08 and 1 K and power-law susceptibility between 0.08 and 3 K (ref. 8). Generally (as indeed has been observed for $CeCu_{6-x}Au_x$), such non-Fermi liquid regime is related to a quantum critical point, i.e. to a 2nd order phase transition typically from paramagnetism to antiferromagnetism at around $T = 0$ K as a function of a control parameter such as composition, pressure or magnetic field. Among the most common factors that are currently considered to

influence the appearance of such non-Fermi liquid behaviour are disorder, magnetic anisotropy, strong Kondo screening. Interestingly, in the case of $CeCu_{6-x}Au_x$, it was found (ref. 9) that the structural distortion (discussed previously for the parent compound $CeCu_6$) competes with antiferromagnetism, i.e. the structural distortion and the long-range antiferromagnetic order disappear at exactly the same critical concentration $x_c = 0.13$ where non-Fermi liquid behaviour was observed. This observation strongly suggests that the lattice distortion and the concomitant structural fluctuations at $x_c = 0.13$, which are a source of disorder, are also a source of the non-Fermi liquid behaviour of the $CeCu_{5.9}Au_{0.1}$. Signatures of such non-Fermi liquid behaviour are found at the temperature dependence of magnetic susceptibility, resistivity and specific heat of heavy-fermion materials. Considerably fewer experimental data exist on the temperature dependence of the thermoelectric coefficients (thermopower, Nerst coefficient) of non-Fermi liquid systems. A few available results reveal unexpectedly enhanced or reduced thermoelectric coefficients. Therefore, the relationship between non-Fermi liquid behaviour, disorder (including lattice distortions and concomitant structural fluctuations) and enhanced or not thermoelectric properties is currently an open question in the physics of heavy-electron materials. The line of research presented here has been conceived as a step in this direction.

Recently, substitution of Cu by Sn has been found to significantly reduce the thermopower of $CeCu_6$ (ref. 10). Moreover, a crossover from Kondo lattice to antiferromagnetic ordering has been reported to take place in $CeCu_{6-x}Sn_x$ (ref. 10). The phases $CeCu_{5.25}Sn_{0.75}$ and $CeCu_5Sn$ order antiferromagnetically at T_N = 4 K and 10 K respectively. In order to investigate whether the interplay between structural and magnetic degrees of freedom (discussed above for Au-doped $CeCu_6$) is a generic characteristic of doped-$CeCu_6$ and gain insight on the factors that are important for its low-temperature transport, magnetic and thermoelectric properties, we investigated the phases $CeCu_{6-x}Sn_x$ for x = 0, 0.25, 0.65, 0.75, 0.85 and 1. Following the earlier report on the properties of $CeCu_{6-x}Sn_x$ phases (ref. 10), we present here an investigation combining a structural analysis by powder neutron diffraction with specific heat measurements. We mostly focus our study

to the samples with high Sn-content where an antiferromagnetic order has been reported to take place.

2. Experimental

2a. Sample preparation

The samples were prepared by melting the starting metals (cerium 99.8%, electrolytic copper 99.99% and tin 99.99%) in an electric arc furnace. The nominal composition of the $CeCu_{6-x}Sn_x$ samples was: x = 0, 0.25, 0.65, 0.75, 0.85 and 1.0. The obtained materials were annealed at 500°C for 720 h in vacuum. The quality of the samples was checked using conventional powder X-ray diffraction.

2b Powder neutron diffraction

The powder neutron diffraction experiments were performed on the D1B instrument (CRG) (ref. 11) at the Institut Laue Langevin (ILL), Grenoble (France). During the neutron diffraction measurements, a cylindrical vanadium sample holder of 6 mm inner diameter was used. The diffraction patterns were recorded over an angular range 2θ of 80° using a multidetector with a step of 0.2° between each of the 400 ^{3}He detection cells. The neutron wavelength was λ = 2.52 Å selected by the (002) Bragg reflection of a pyrolitic graphite monochromator with take off angle of 2θ = 44.2°. The measurements were carried out in the temperature range 10 to 300 K with a step of 7 K using the orange ILL cryostat. For the refinement of the data collected on D1B, a small angular region around 2θ = 72°, containing a peak originating from the vanadium tail of the cryostat, was excluded.

The data were analysed by the Rietveld structure refinement program FULLPROF (ref. 12). The agreement factors used in this article are defined as $\chi^2 = R_{wp} / R_{exp}$, $R_{exp} = [(N\text{-}P+C)/\Sigma_i\, w_i\, y_i^2]^{1/2}$

and $R_{wp} = \{\Sigma_i\, w_i\, (y_i\text{-}y_{ci})^2 / \Sigma_i\, w_i\, y_i^2\}^{1/2}$ where y_i and y_{ci} are the observed and calculated counts at the ith step of the pattern respectively and w_i is the weights of the observations. $N\text{-}P\text{+}C$ is the number of degrees of freedom (N is the number of points in the pattern, P the number of refined parameters and C the number of constraint functions). The Bragg agreement factor is defined as $R_B = \Sigma_k\, |I_k\text{-}I_{ck}| / \Sigma_k\, |I_k|$ where I_k and I_{ck} are the observed and the calculated integrated nuclear intensity at the kth reflection respectively. Guidelines of the Rietveld refinement can be found elsewhere (ref. 13). The neutron scattering lengths used were $b_{Ce} = 0.484\ 10^{-14}$ m, $b_{Sn} = 0.6225\ 10^{-14}$ m and $b_{Cu} = 0.7718\ 10^{-14}$ m, values taken from reference 14.

2c. Specific heat measurements

The specific heat of the $CeCu_{6-x}Sn_x$ (x = 0, 0.25, 0.65, 0.75, 0.85 and 1.0) samples was measured using the Physical Property Measurement System (PPMS-14, Quantum Design), installed at DCMP, Charles University, Prague (Czech Republic). The relaxation 2-τ fitting method was used for the measurement. The experiment was performed in the temperature range 0.35 to 40 K and in magnetic fields up to 10 T. The mass of the samples was in the range of 1 to 5 mg. The He-3 option (QD) was installed to reach temperatures down to 350 mK.

3. Results and discussion

3a. Crystal structure

The existence of the series RCu_5Sn (R = La, Ce, Pr, Nd and Sm) has been first reported by Skolozdra and co-workers (ref. 15) and independently by Fornasini et al. (ref. 16). According to Skolozdra, the compounds RCu_5Sn adopt the $CeCu_6$ type-structure (ref. 17) but without forming a complete solid solution between RCu_6 and RCu_5Sn. Conventional powder X-ray diffraction of the $CeCu_{6-x}Sn_x$ (x = 0, 0.25, 0.65, 0.75, 0.85 and 1) compounds investigated here, revealed only traces

of elemental Sn in the samples with higher Sn content and only traces of CeO_2 in the $CeCu_6$ sample. The $CeCu_{6-x}Sn_x$ compounds are found to crystallize in the orthorhombic symmetry adopting the P*nma* space group similarly to the $CeCu_5Au$ compound (ref. 18).

The lattice parameters deduced from the refinement of the neutron diffraction data of the $CeCu_{6-x}Sn_x$ (x = 0, 0.25, 0.65. 0.75, 0.85, 1) compounds are summarized in Table I. As can be seen from this table, the lattice expands with the substitution of Cu by Sn, which indicates that the substitution is equivalent to negative chemical pressure on the lattice. The composition x dependencies of the lattice parameters a, b and c and of the volume V are given in Figure I. The b lattice parameter is almost insensitive to the substitution of Cu by Sn in the $CeCu_{6-x}Sn_x$ structure. On the contrary, both lattice parameters a and c increase continuously with x; c being by far the most sensitive to the Sn concentration.

We now focus on the crystal structure of the compounds $CeCu_{5.25}Sn_{0.75}$ and $CeCu_5Sn$ which are representative phases in the area of high Sn content, where antiferromagnetic order at low temperatures has been reported (ref. 10). Their crystal structure was investigated in detail above their corresponding Néel temperatures in order to determine the exact site occupancy of Sn in the structure and its influence to the other structural parameters and to compare it with the structure of the parent compound $CeCu_6$. An example of the Rietveld refinement fit is given in Figure II for $CeCu_{5.25}Sn_{0.75}$ at 5 K. The structural results of the Rietveld refinement of the neutron diffraction data are summarized in Tables II and III for the $CeCu_{5.25}Sn_{0.75}$ and $CeCu_5Sn$ respectively. It is unambiguously deduced from the refinements that the Sn atoms exhibit a strong preference for the Cu 4*c* site of the $CeCu_6$ structure. Such preference for the 4*c* site confirms earlier reported results obtained by X-ray diffraction investigations (ref. 15, 16). This atomic position is the site with the highest coordination number: 14 atoms. Unlike the other Cu sites which are surrounded by 12 to 13 near neighbour atoms (3 of which are Ce atoms), the site filled by Sn is surrounded by 14 near neighbours: 10 Cu and 4 Ce atoms. Consequently, the occupation of this site by Sn maximizes the number of Ce-Sn bonds. Furthermore, it is worth to recall that both Sn atoms (like Au) are larger

than copper; this size difference may favour such preferential substitution scheme. In order to test this assumption, a calculation of the atomic cell volume of the $CeCu_6$ type structure has been carried out. The Wigner-Seitz (W.S.) atomic cell volume of the Voronoi-Dirichlet polyhedron around an atomic site has been calculated as described elsewhere (ref. 19-22). The metallic atomic radii used are the following: r_{Cu} = 1.28 Å, r_{Sn} = 1.60 Å, r_{Ce} = 1.846 Å according to the calculations of reference 23. The available atomic cell volume calculated for each atomic site is summarized in Table III for $CeCu_5Sn$. It is clear that the position preferentially occupied by Sn atoms is the one exhibiting the larger volume, thus favouring the accommodation of large atoms such as Sn or Au. Similar calculations on the pure $CeCu_6$ compounds confirm that the position preferred by Sn exhibits the larger W.S. atomic cell volume: 13.7Å^3 against only 12.4 Å^3 and about 12 Å^3 for the Cu_8*d* and the two other Cu_4*c* site respectively. Upon substituting Sn for Cu, both the expansion of the unit cell as well as the evolution of the coordinates of the atomic positions permit to accommodate the large Sn atom in the $CeCu_6$ type crystal structure. Indeed, all atoms of $CeCu_{6-x}Sn_x$ are in general positions of the P*nma* space group and therefore the coordinates of the atomic positions are allowed to change. Thus, for the end-member $CeCu_5Sn$ the volume available for the Sn site reaches 20.79 Å^3.

We now turn to the temperature dependence of the crystal structure of the compounds $CeCu_{5.25}Sn_{0.75}$ and $CeCu_5Sn$. Our Rietveld refinements of the powder neutron diffraction data, collected in the temperature range from 4 to 300 K, demonstrate the absence of any structural phase transition for the investigated compositions. Similar behaviour was previously observed for the $CeCu_{6-x}Au_x$ materials with x>0.13 (ref. 24, 25). Therefore, the substitution of Cu by Sn suppresses the orthorhombic to monoclinic transition, known to occur in the pure $CeCu_6$ phase and in the $CeCu_{6-x}Au_x$ phases with x<0.13 (ref. 24, 25). The temperature dependence of the lattice parameters below RT is plotted in Figure III for x = 1. As expected, the increase of the temperature from 4 to 300 K leads to an expansion of the unit cell volume of a bit more than 5 Å^3 for $CeCu_5Sn$. It is worth to note that no anomalous behaviour is observed in this thermal evolution, thus confirming the

absence of any structural phase transition within this temperature range. The thermal expansion of the lattice parameters *a* and *c* is very similar, i.e. they both expand of about 0.035 Å upon increasing the temperature from 5 K to RT. The increase of the *b* parameter is significantly smaller and reaches 0.022 Å. It is worth to mention that in spite of the similar thermal expansion of *a* and *c*, observed in Figure III, given that *c* is much larger than *a* (about 10 Å and 8 Å respectively), the expansion of the cell is larger in *a* direction relatively to *c* direction. Indeed, an increase of 0.42%, 0.43% and 0.33% is observed for *a*, *b* and *c* respectively. This observation demonstrates that the temperature induced expansion of the unit cell, involves all the lattice parameters and it is not isotropic.

3b. Specific heat measurements

The specific heat C_p of $CeCu_{6-x}Sn_x$ (x = 0, 0.25, 0.65, 0.75, 0.85, 1) has been measured at zero magnetic field down to temperature of 0.4 K. The specific heat of $CeCu_6$, plotted as C_p/T versus T^2 (Fig. IV), exhibits a rapid increase of C_p/T below ≈ 7 K which is quite typical of many heavy-fermion materials and is in agreement with the previous studies of $CeCu_6$ (see for example ref. 1). The sample having low Sn content x = 0.25 exhibits an enhancement of the C_p/T value (Fig. V) at low temperatures compared to $CeCu_6$. Such behaviour can be suppressed by applying a magnetic field. A linear fit of the low-temperature data C_p/T versus T^2 data of $CeCu_6$ and $CeCu_{5.75}Sn_{0.25}$ and extrapolation of the C_p/T value down to 0 K leads to a γ value of about 2.550(73) J/mole K^2 for $CeCu_{5.75}Sn_{0.25}$ that is clearly enhanced compared to $\gamma \approx$ 1.386(7) J/mole K^2 obtained here for the reference polycrystalline compound $CeCu_6$ and to $\gamma \approx$ 1.6 J/mole K^2 obtained from the literature for the reference single crystalline compound $CeCu_6$.

Figure VI shows the zero-field evolution of C_p as a function of T in the temperature range 0.4 – 20 K of the series $CeCu_{6-x}Sn_x$ (x = 0, 0.65, 0.75, 0.85, 1). For higher Sn concentration x = 0.65, 0.75, 0.85 and 1 an anomaly of C_p/T appears, revealing the occurrence of a magnetic order in these compounds, which has been already observed by magnetic susceptibility measurements at earlier studies (ref. 10). We now focus on the broad peak of the C_p/T versus T curve observed at T_N.

This peak is more broad for x = 0.65 and less broad for 0.85. Samples with x = 0.65, 0.75, 0.85 and 1 present magnetic order at T_N = 3.5, 3.7, 4.0 and 4.2 K, respectively. This reveals an increase of the antiferromagnetic ordering temperature T_N with the increase of the Sn content. Long-range antiferromagnetic order has also been reported to occur in the $CeCu_{6-x}Au_x$ compounds for $0.1 \leq x \leq 1$ as mentioned in the introduction.

In order to further understand the nature of the strong electron-electron interactions in doped $CeCu_6$ in general and in $CeCu_{6-x}Sn_x$ in particular, we investigated the influence of an applied magnetic field on the specific heat of $CeCu_{6-x}Sn_x$ samples with high Sn content. The results are plotted in Figures VII, VIII and IX for x = 0.65; 0.75; and 1 respectively. There is a clear decrease of the specific heat at T_N caused by the applied magnetic field. This effect is even more pronounced for $CeCu_{6-x}Sn_x$ with x = 0.65 since at 10 T the broad peak at T_N is almost suppressed, whereas the sensitivity to the applied magnetic field of the compounds $CeCu_{6-x}Sn_x$ with x = 0.75 and 1 is much weaker. These results reveal that the higher the Sn content in $CeCu_{6-x}Sn_x$, the weaker the sensitivity of C_p to an applied magnetic field. In other words, in an oversimplified picture where disorder is considered to be the same for all samples, the higher the Sn content, the higher has to be the applied magnetic field in order to suppress the magnetic transition.

The evolution of magnetism of $CeCu_{6-x}Sn_x$ as a function of x and/or the applied magnetic field is a result of a delicate balance between various competing interactions which involve its very basic physics, energy scales and crystal chemistry. In an ordered material such as $CeCu_6$ or $CeCu_5Sn$, the exchange interaction J (which couples the local spins to the conduction electrons) and the density of conduction electrons at the Fermi level influence both the Kondo temperature, T_K, below which compensation of the local moments by the cloud of conduction electrons occurs, and the Ruderman-Kittel-Kasuya-Yosida (RKKY) temperature, T_{RKKY}, which characterizes the moment-moment interaction in the material. Consequently, in $CeCu_6$ and in $CeCu_5Sn$ the exchange interaction J and the density of conduction electrons control the obvious competition between the single-site Kondo screening and inter-site RKKY spin coupling, i.e. between the low-temperature

compensated state and the magnetically ordered state of the uncompensated moments. This competition is quite complex because the two energy scales T_K and T_{RKKY} have different dependences not only on the density of conduction electrons at the Fermi level but also on $|J|$: T_K depends exponentially on $|J|$ and T_{RKKY} changes as $|J|^2$. We note that $T_K = (1/N(E_F))\exp(-1/N(E_F)J)$ and $T_{RKKY} = -J^2 N(E_F)$, where $N(E_F)$ is the density of the electrons at the Fermi level. Turning now to $CeCu_{6-x}Sn_x$, it is instructive to recall (cf. Section 3*a*) that the substitution of Cu by Sn in $CeCu_6$ takes place at a special Cu site which is next to each of the four Ce atoms in the unit cell, maximizing in this way the number of Ce-Sn bonds. Such substitution and the resulting structural changes modify the exchange parameter $|J|$, change the density of conduction electrons and introduce disorder. In the $CeCu_{6-x}Sn_x$ phases where disorder effects are quite pronounced, the competition between Kondo screening and RKKY interaction is very complex. It has been demonstrated by several theoretical and experimental studies on a wide variety of heavy-fermion systems that modest disorder leads to modest variations of J which, because it is amplified exponentially, can lead to wide distributions of T_K and thus to dramatic changes of the low-temperature properties of the heavy-fermion material. We believe that, given that the electronic state of Ce does not vary much because of the substitution of Cu by Sn (ref. 10), the evolution of magnetism as a function of x in $CeCu_{6-x}Sn_x$ and its sensitivity or not to the applied magnetic field results from the complex competition between Kondo and RKKY interactions. This competition is influenced by the changes of $|J|$ (which in turn are caused by the variations of the interatomic distances, the type of first neighbours of Ce and the disorder) and by the variations of the density of the conduction electrons in the alloyed samples.

3. Concluding remarks

$CeCu_{6-x}Sn_x$ is an interesting system to investigate the competition between the two basic types of interactions in heavy-fermion systems, the Kondo and RKKY interaction. Our study,

focused mostly on the highly doped samples (where antiferromagnetic order takes place), revealed that no structural phase transition occurs in these samples as a function of x or temperature. However, the substitution of Cu by Sn increases considerably the cell volume (because the Sn atom is bigger than Cu), provides higher concentration of conduction electrons (because Sn has more valence electrons than Cu), and modifies the local structure and chemistry around the Ce atoms (since Sn occupies preferentially the special Cu site which is next to each of the four Ce atoms in the unit cell). The result of these three effects is the progressive dominance of the RKKY interaction over the Kondo interaction and thus the establishment of a long-range antiferromagnetic order of the uncompensated moments. This order is most robust in the ordered material $CeCu_5Sn$ and therefore higher magnetic fields are required to suppress the magnetic transition.

While further experiments on the crystal/magnetic structure and on the physical properties as well as band structure calculations would be valuable to establish an accurate Doniach's phase diagram of T vs x of $CeCu_{6-x}Sn_x$, the present results unravelled a very interesting structural chemistry behind the physics of this system and a remarkable interplay between its composition, structure and magnetism. Whether this interplay can be further tuned by control parameters like pressure or higher magnetic fields remains an open interesting question.

Acknowledgements

The work of J. P. and P. J. is a part of the research plan MSM 0021620834 that is financed by the Ministry of Education of the Czech Republic. E.G.M. and O.I. thank GSRT and Égide respectively for financial support through the French-Greek cooperation program PLATON #11202UA and ILL for beam time at the instrument D1B (CRG).

x	a (Å)	b (Å)	c (Å)	V (Å^3)
0	8.117(1)	5.106 (7)	10.182 (2)	422.0
0.25	8.218 (1)	5.079 (2)	10.281 (1)	429.2
0.65	8.330 (1)	5.067 (1)	10.551 (2)	445.4
0.75	8.319 (2)	5.073 (2)	10.520 (3)	444
0.85	8.328 (1)	5.069 (1)	10.595 (1)	447.2
1	8.323 (1)	5.064 (1)	10.597 (1)	447.6
1.2 (ref. 15)	8.342 (1)	5.067 (5)	10.651 (10)	450.2

Table I: Lattice parameters of the $CeCu_{6-x}Sn_x$ compounds at RT.

Atom	site	x	y	z	Occupancy
Ce	4*c*	0.230 (3)	0.25	0.561 (2)	1
Cu1	8*d*	0.0685 (9)	0.4976 (22)	0.3078 (8)	1
Cu2	4*c*	0.0513 (18)	0.25	0.1059 (16)	1
Cu3	4*c*	0.3105 (20)	0.25	0.2466 (12)	1
Cu4	4*c*	0.4137 (20)	0.25	0.0213 (13)	1
Sn5/Cu5	4*c*	0.1416 (19)	0.25	0.8660 (15)	0.70/0.30(7)

Table II: Structural parameters of $CeCu_{5.25}Sn_{0.75}$ deduced from the refinement of the neutron powder diffraction data collected at 5 K. The standard deviations are given in parenthesis. Space group: P*nma*; lattice parameters: a = 8.297(1) Å, b = 5.067(1) Å, c = 10.555(2) Å. Rietveld refinement agreement factors: R_p = 7.81%, R_{wp} = 7.60%, R_B = 2.96%.

Atom	site	W.S. ($Å^3$)	Near neighbours	x	y	z	occupancy
Ce	4*c*	31.3	15 Cu + 4 Sn	0.259 (3)	0.25	0.557 (3)	1
Cu1	8*d*	11.85	7 Cu + 2 Sn + 3 Ce	0.070 (1)	0.4936 (19)	0.3075 (8)	1
Cu2	4*c*	12.2	7 Cu + 3 Sn + 3 Ce	0.0664 (15)	0.25	0.0977 (13)	1
Cu3	4*c*	12.1	7 Cu + 2 Sn + 3 Ce	0.3253 (20)	0.25	0.2467 (12)	1
Cu4	4*c*	11.6	8 Cu + 1 Sn + 3 Ce	0.4215 (23)	0.25	0.0101 (11)	1
Sn5 /Cu5	4*c*	20.8	10 Cu + 4 Ce	0.1462 (18)	0.25	0.8556 (14)	0.87/0.13(10)

Table III: Structural parameters of $CeCu_5Sn$ deduced from the neutron powder diffraction data collected at 5 K. The standard deviations are given in parenthesis. Space group: P*nma*; lattice parameters: a = 8.339(2) Å, b = 5.061(1) Å, c = 10.651(3) Å; Rietveld refinement agreement factors R_p = 7.64%, R_{wp} = 7.38%, R_B = 4.00%. The sample contains two phases: 97% $CeCu_5Sn$ and 3% Sn. The nearest neighbours and the Wigner-Seitz atomic cell volume are given for each atomic position.

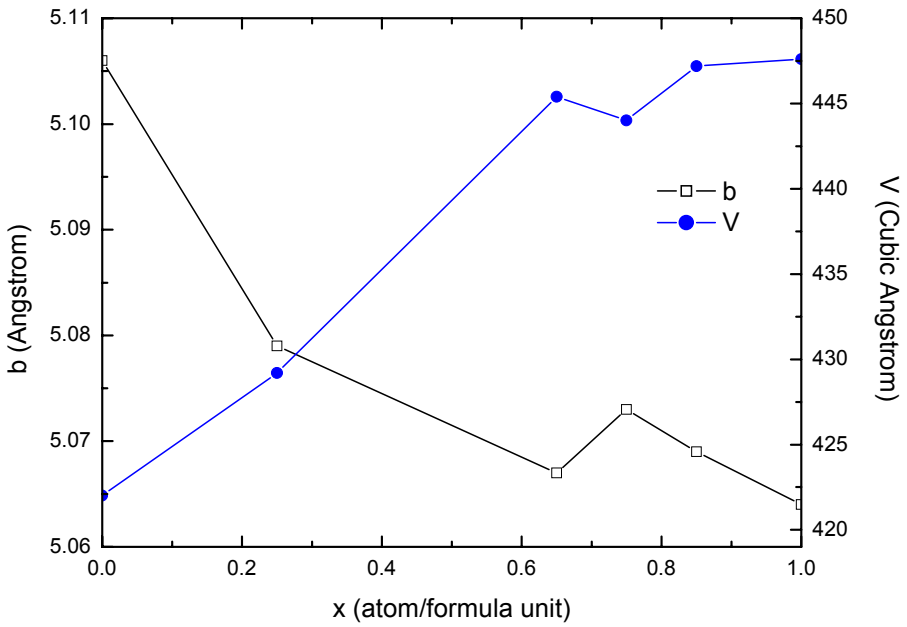

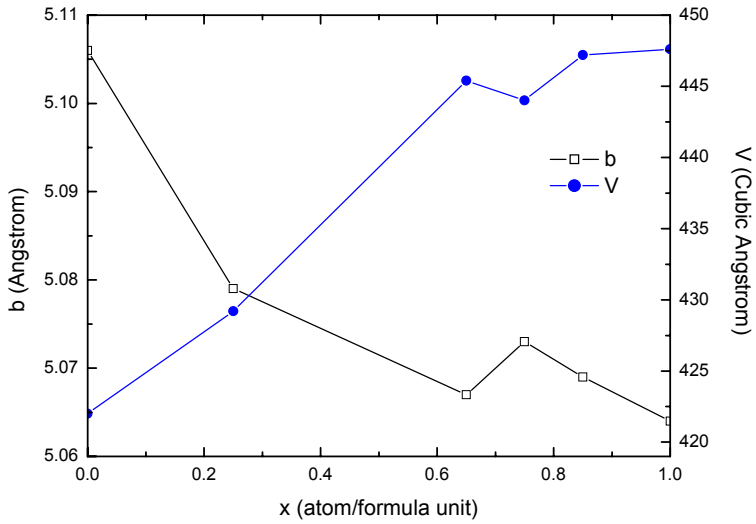

Fig. I: Composition *x* dependence of the lattice parameters *a, b* and *c* and of the unit cell volume *V* of the $CeCu_{6-x}Sn_x$ compounds. Estimated standard deviations are listed in Table I.

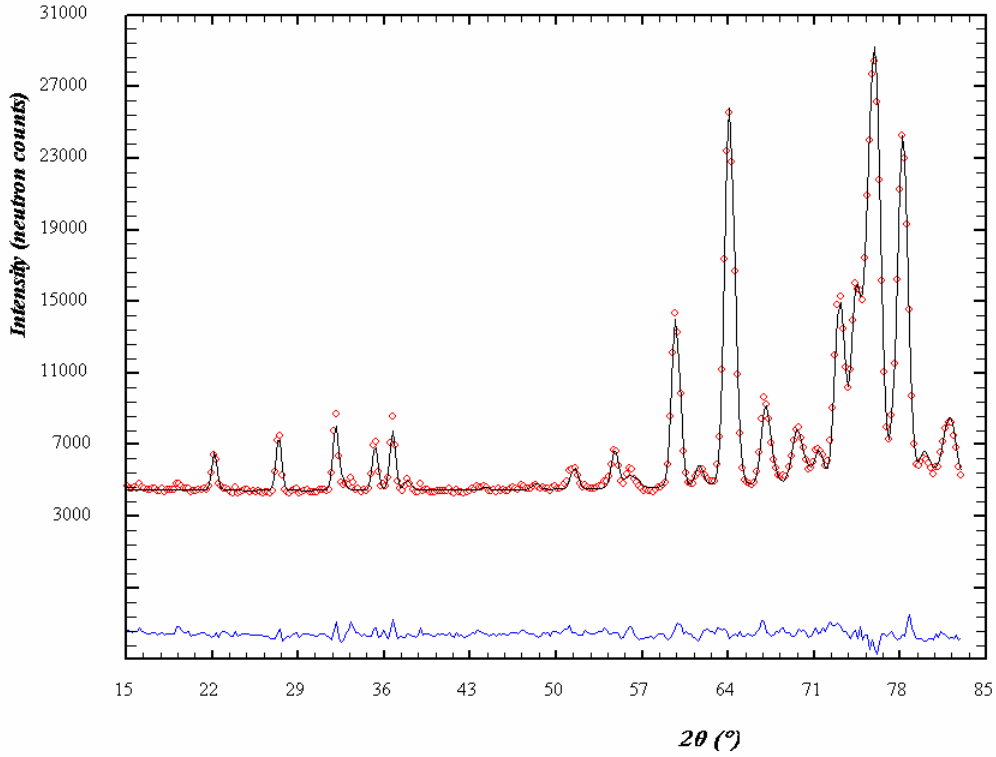

Fig. II: Neutron powder diffraction pattern of $CeCu_{5.25}Sn_{0.75}$ at 5 K. The dots and the full curve refer to the recorded pattern and the calculated fit respectively. The difference pattern is plotted in the lower part of the figure on the same scale. The Rietveld agreement factors are R_p = 7.81%, R_{wp} = 7.60%, R_B = 2.96 %.

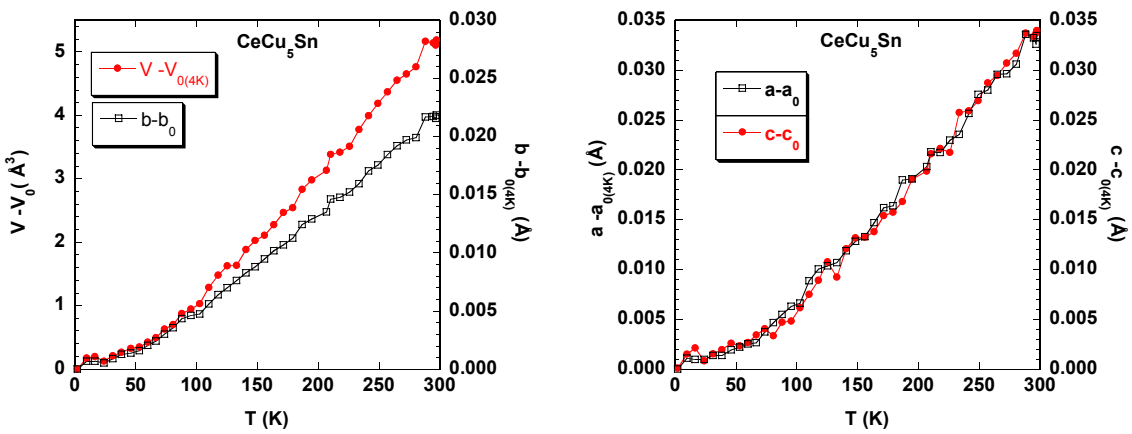

Fig. III. Temperature dependence of the lattice parameters of $CeCu_5Sn$.

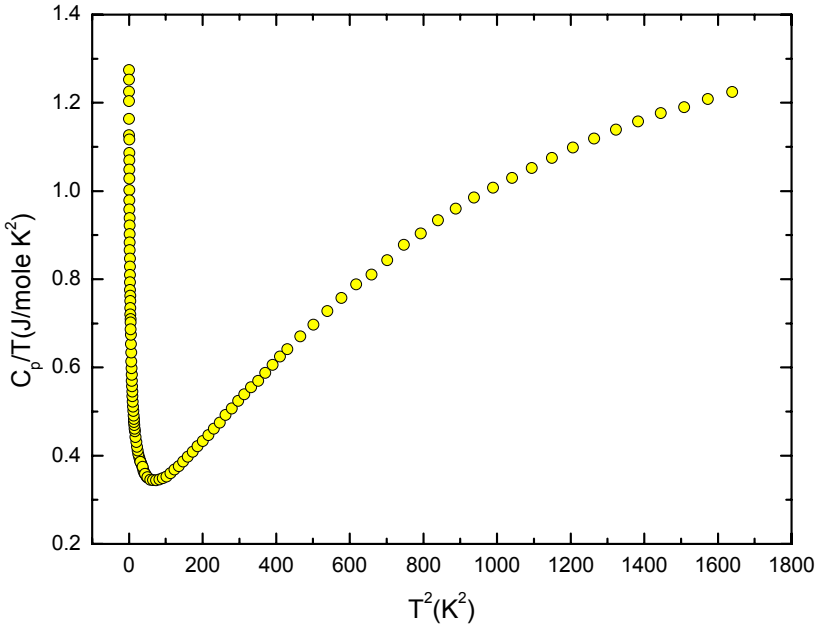

Fig. IV. Specific heat of polycrystalline $CeCu_6$ at zero magnetic field.

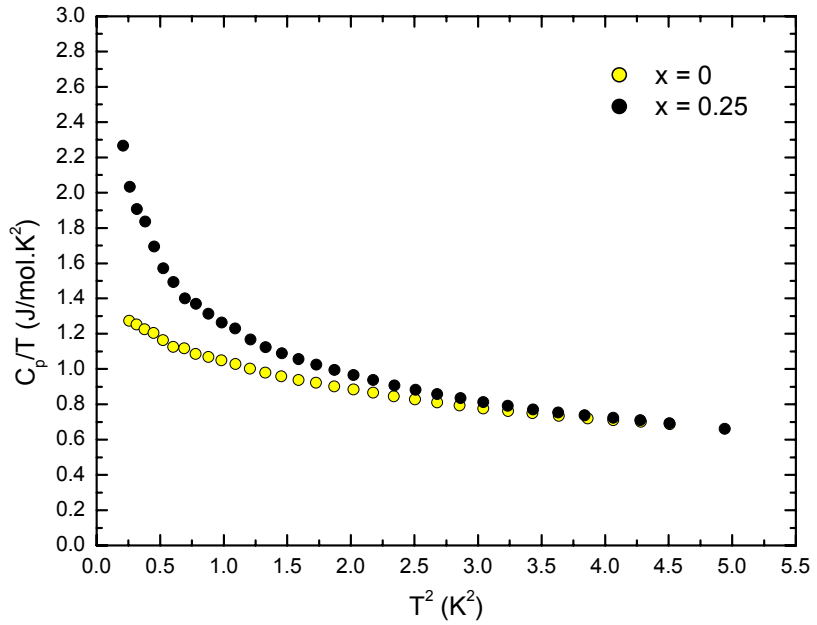

Fig. V: Low temperature specific heat of the $CeCu_{6-x}Sn_x$ compounds with x = 0.25 and x = 0 at zero magnetic field.

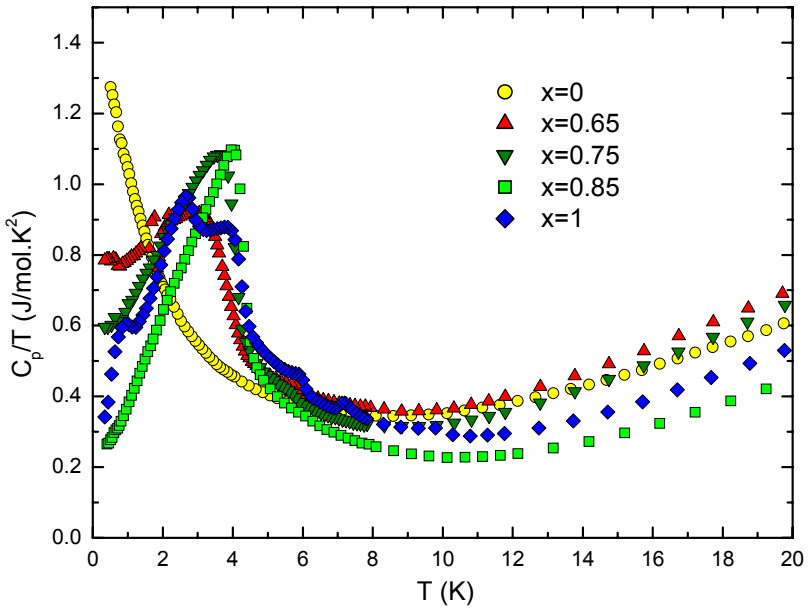

Fig. VI: Comparison of the specific heat of polycrystalline $CeCu_{6-x}Sn_x$ with high Sn content at zero magnetic field. For reference the specific heat of the parent compound $CeCu_6$ is also shown.

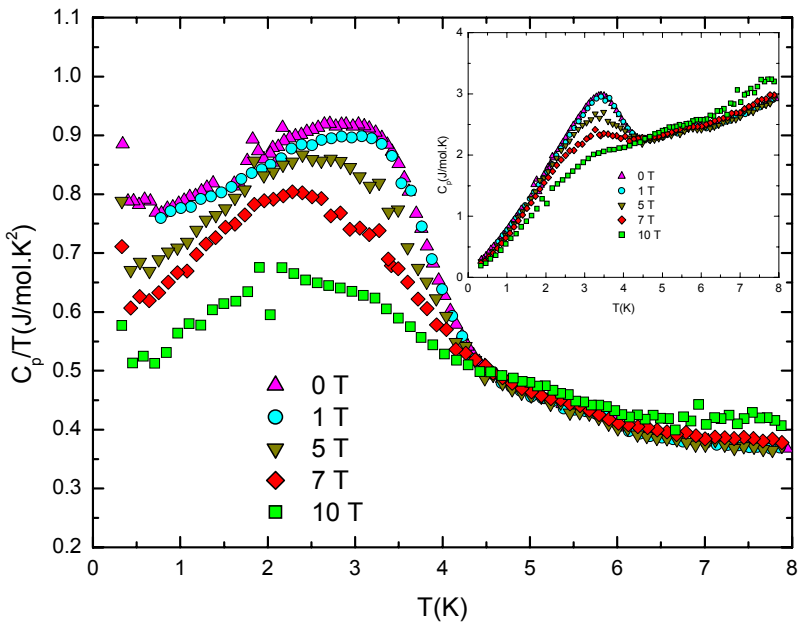

Fig. VII: Evolution of C_p/T versus T of the $CeCu_{5.35}Sn_{0.65}$ for applied magnetic fields of 0, 1, 5, 7 and 10 T. The inset shows the evolution of C_p versus T for the same fields.

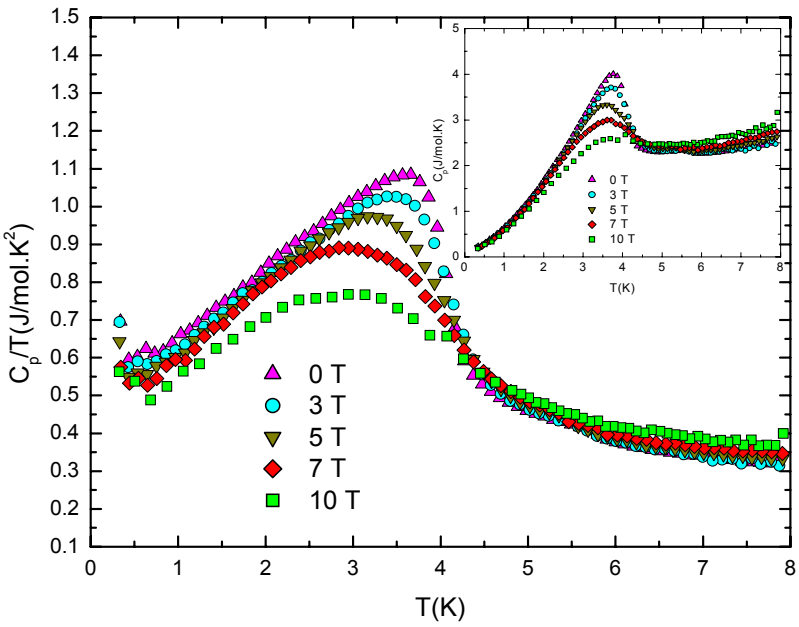

Fig. VIII: Evolution of C_p/T versus T of the $CeCu_{5.25}Sn_{0.75}$ for applied magnetic fields of 0, 3, 5, 7 and 10 T. The inset shows the evolution of C_p versus T for the same fields.

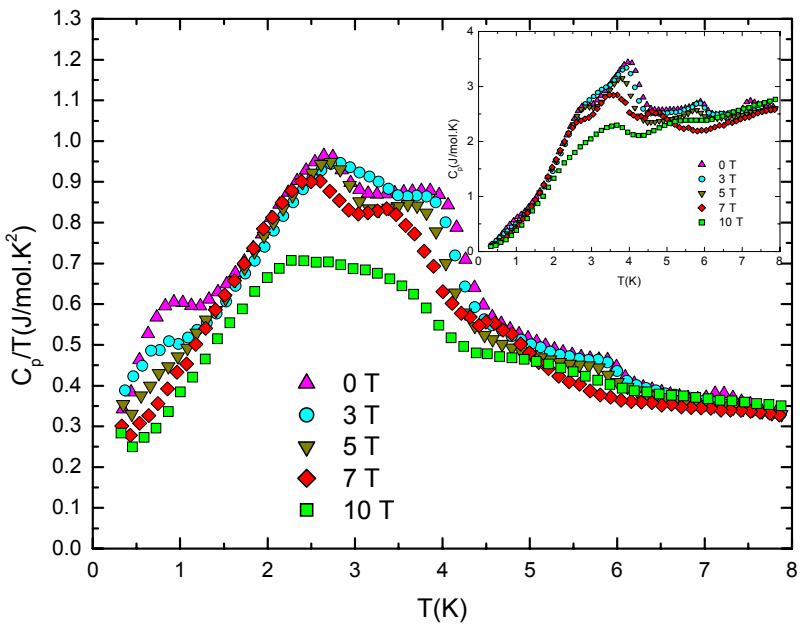

Fig. IX: Evolution of C_p/T versus T of the $CeCu_5Sn$ for applied magnetic fields of 0, 3, 5, 7 and 10 T. The inset shows the evolution of C_p versus T for the same fields.

References

1. G. R. Steward, Z. Fisk, M. Wire, *Phys. Rev. B* **30**, 482 (1984).

2. J. Rossat-Mignod, L. P. Regnault, J. L. Jacoud, C. Vettier, P. Lejay, J. Flouquet, E. Walker, D. Jaccard, A. Amato, *J. Magn. Magn. Mater.* **76–77**, 376 (1988).

3. H. Tsujii, E. Tanaka, Y. Ode, T. Katoh, and T. Mamiya, S. Araki, R. Settai, and Y. Ōnuki, *Phys. Rev. Lett*. **84**, 5407 (2000).

4. M. L. Vrtis, J. D. Jorgensen, D. G. Hinks, *Physica* **136B**, 489 (1986).

5. E. Gratz, E. Bauer, H. Nowotny, H. Mueller, S. Zemirli, B. Barbara, *J. Magn. Magn. Mater.* **63 & 64**, 312 (1987).

6. M. L. Vrtis, J. D. Jorgensen, D. G. Hinks, *J. Sol. State. Chem.* **84**, 93 (1990).

7. A. Schroëder, G. Aeppli, R. Coldea, M. Adams, O. Stockert, H. v. Löhneysen, E. Bucher, R. Ramazashvili, P. Coleman, *Nature* **407,** 351 (2000) and references therein.

8. H. v. Löhneysen, S. Mock, A. Neubert, T. Pietrus, A. Rosch, A. Schröder, O. Stockert, U. Tutsch, *J. Magn. Magn. Mater.* **177-181**, 12 (1998) and references therein.

9. R. A. Robinson, D. J. Goossensa, M. S. Torikachvili, K. Kakuraic, H. Okumurac, *Physica B* **385–386**, 38 (2006).

10. O. Isnard, J. Pierre, D. Fruchart, L. P. Romaka, R. V. Skolozdra, *Solid State Commun.* **113,** 335 (2000).

11. ILL yellow book; available at www.ill.fr

12. J. Rodriguez-Carvajal, Fullprof Suite, available at http://www.ill.eu/sites/fullprof/.

13. L. B. McCusker, R. B. Von Dreele, D. E. Cox, D. Louër, P. Scardi, *J. Appl. Cryst.* **32**, 36 (1999).

14. V. F. Sears, *Neutron News* **3,** 26 (1992).

15. R. V. Skolozdra, L. P. Romaka, L. G. Akselrud, J. Pierre, *J. Alloys and Compds* **262-263,** 346 (1997).

16. M. L Fornasini, R. Marazza, D. Mazzone, P. Riani, G. Zanicchi, *Z. Kristallog*r. **213**, 108 (1998).

17. D. T. Cromer, A. C. Larson, B. R. Roof Jr., *Acta Cryst.* **13**, 913 (1960).

18. M. Rück, G. Portisch, H. G. Schlager, M. Sieck, M. v Löhneysen, *Acta Cryst.* **B49,** 936 (1993).

19. L. Gelato, *J. Appl. Cryst.* **14**, 151 (1981).

20. B. J. Gellaty, J. L. Finney, *J. Non-Cryst. Solids,* **50**, 313 (1982).

21. W. Fischer, E. Koch, E. Hellner, *Neues Jahrb. Mineral. Montash,* 227 (1971).

22. O. Isnard, D. Fruchart, *J. Alloys Compds* **205**, 1-15 (1994).

23. E. T. Teatum, K. A. Gschneidner Jr, J. T. Waber "Compilation of calculated data useful in predicting metallurgical behaviour of elements in binary alloy systems" Los Alamos Report, LA-4003, University of California 58 (1968).

24. K. Grube, W. H. Fietz, U. Tutsch, O. Stockert, H. v. Löhneysen, *Phys. Rev. B* **60**, 11947 (1999) and references therein.

25. H. v. Löhneysen, A. Schröder, O. Stockert, *J. Alloys Comp.* **303–304,** 480 (2000) and references therein.